Research Article **Open Access**

Jinn-Liang Liu*

A Quantum Corrected Poisson-Nernst-Planck Model for Biological Ion Channels

DOI 10.1515/mlbmb-2015-0005
Received April 15, 2015; accepted July 29, 2015

Abstract: A quantum corrected Poisson-Nernst-Planck (QCPNP) model is proposed for simulating ionic currents through biological ion channels by taking into account both classical and quantum mechanical effects. A generalized Gummel algorithm is also presented for solving the model system. Compared with the experimental results of X-ray crystallography, it is shown that the quantum PNP model is more accurate than the classical model in predicting the average number of ions in the channel pore. Moreover, the electrostatic potential has been found to reach as high as 19% difference between two models around the charged vestibule which has been shown to play a significant role in the permeation of ions through ion-selective ligand-gated or voltage-activated channels. These results indicate that the QCPNP model may be considered as a more refined continuum model that can be incorporated into a multi-scale electrophysiology modeling.

Keywords: Ion channel; Poisson-Nernst-Planck model; Bohm's quantum potential

MSC: 35Q92, 53Z05, 65C20, 70E55, 92B05

1 Introduction

Ion channels are porous proteins across cell membranes that control many biological functions ranging from signal transfer in the nervous system to regulation of secretion of hormones. Understanding the mechanism of ionic flows within a channel as a function of ionic concentration, membrane potential, and the structure of the channel is a central problem in molecular biophysics [16].

The Poisson-Nernst-Planck (PNP) model proposed by Eisenberg and coworkers [2, 6, 11, 13, 18, 26] for simulating the ionic flow in an open ion channel is one of commonly used models in theoretical and computational studies of biological ion channels. Ion channels are nanoscale conduits through which specific ions move. We present here a quantum hydrodynamic model that extends the classical PNP model to include Bohm's quantum potential [3] that corrects the electric field in the drift process of the ionic movement. It is hence called a quantum corrected PNP (QCPNP) model which is then transformed into a self-adjoint and semilinear system of PDEs as that for semiconductor device simulations proposed by Slotboom [31]. It is well-known [1, 4] that the Slotboom formulation may cause overflow problems in computer implementation if the applied voltage is too large. Fortunately, the biasing voltage for biological ion channels is in general below 200 millivolts [14, 16] which is much less than that of semiconductor devices. The self-adjoint formulation provides many appealing features for both mathematical analysis [1, 20, 21] and numerical simulations such as global convergence by monotone iterative methods [7], optimal convergence in the sense of Gummel's iteration [9], highly parallelizable and fast iterative solution [22], and a single finite-element subspace approximation to all PDEs of the model [7, 8].

As an example to study the quantum effect on ionic currents in a physiologically important channel, we consider the K channel in KCl solutions using the TRBDF2 method as illustrated in [14]. Compared with the

***Corresponding Author: Jinn-Liang Liu:** Department of Applied Mathematics, National Hsinchu University of Education, Hsinchu 300, Taiwan, E-mail: jinnliu@mail.nhcue.edu.tw

BY-NC-ND © 2015 Jinn-Liang Liu, licensee De Gruyter Open.
This work is licensed under the Creative Commons Attribution-NonCommercial-NoDerivs 3.0 License.

experimental results of X-ray crystallography, it is shown that the quantum PNP model is more accurate than the classical model in predicting the average number of ions in the channel pore. Moreover, the electrostatic potential has been found to reach as high as 19% difference between two models around the charged vestibule which has been shown to play a significant role in the permeation of ions through ion-selective ligand-gated or voltage-activated channels [5, 19]. These results indicate that the QCPNP model may be considered as a more refined continuum model that can be incorporated into a multi-scale electrophysiology modeling [12, 30].

2 A Quantum Corrected Poisson-Nernst-Planck Model

The quantum potential formulation [3] of the de Broglie-Bohm theory is quite useful to describe particles in motion with precisely definable trajectories and to infer Newtonian mechanics from Bohmian mechanics in the classical limit [17]. The quantum potential is a first order correction to the classical potential and is expressed in terms of the Laplacian of the square root of the probability density of particles. Adding this potential to the drift process of ions within a biological channel, the steady-state Poisson-Nernst-Planck model is extended to

$$\nabla \cdot \mathbf{j}_i = 0, \quad \mathbf{j}_i = -D_i \left[\nabla C_i + \beta_i C_i \nabla(\phi + \psi_i^{\pm})\right], \tag{2.1}$$

$$-\nabla \cdot (\epsilon \nabla \phi) = q_p C_p + \textstyle\sum_i q_i C_i, \tag{2.2}$$

where C_i is the concentration of an ion species i carrying charge q_i (for example, $q_{K^+} = +1e$, $q_{Cl^-} = -1e$), $\mathbf{j}_i$ the concentration flux, D_i the spatially dependent diffusion coefficient, $\beta_i = q_i/(k_B T)$, k_B the Boltzmann constant, T the absolute temperature, ϕ the electrostatic potential, ϵ the dielectric coefficient, q_p the background fixed charge on the channel protein (for example, $q_p = -4e$ [14]), C_p the (known) concentration of charged atoms in the protein, and e the proton charge. The quantum potential of an ion species i is defined by

$$\psi_i^{+} = \frac{-\hbar^2}{2m_i} \frac{\Delta\sqrt{C_i}}{\sqrt{C_i}} \text{ if } q_i > 0, \tag{2.3}$$

$$\psi_i^{-} = \frac{\hbar^2}{2m_i} \frac{\Delta\sqrt{C_i}}{\sqrt{C_i}} \text{ if } q_i < 0, \tag{2.4}$$

where $\hbar$ is the reduced Planck constant and m_i is the ionic mass (for example, $m_K = 39.0983$ and $m_{Cl} = 35.453$ in atomic mass unit). Note that the diffusion coefficient D_i and the parameter β_i are related to the mobility coefficient μ_i by Einstein's relation $\mu_i = |\beta_i| D_i$.

From (2.1), we see that the continuity equation is a fourth order PDE in terms of $\sqrt{C_i}$, which obviously incurs difficulties for solving (2.1) and (2.2) numerically. It is thus natural to treat $\sqrt{C_i}$ as an extra unknown function that satisfies the additional equation

$$\frac{\mp\hbar^2}{2m_i}\Delta\sqrt{C_i} = \sqrt{C_i}\psi_i^{\pm}. \tag{2.5}$$

Note that (2.1), (2.2), and (2.5) are all second order PDEs with respect to the unknown functions C_i, ϕ, and $\sqrt{C_i}$. However, this system of equations is not closed since we still have one more unknown function $\psi_i^{\pm}$ to be determined. Following [7], we resolve this issue by introducing a new variable $\widehat{C}_i$ via the following transformation

$$C_i = \widehat{C}_i \exp(-\beta_i(\phi + \psi_i^{\pm})). \tag{2.6}$$

The concentration flux is then reformulated to

$$\mathbf{j}_i = -D_i \exp(-\beta_i(\phi + \psi_i^{\pm}))\nabla\widehat{C}_i \tag{2.7}$$

and the quantum potential is transformed to

$$\psi_i^{\pm} = \frac{-1}{\beta_i}\left(\ln\left(\sqrt{C_i}\right)^2 - \ln \widehat{C}_i\right) - \phi. \tag{2.8}$$

Consequently, the QCPNP (2.1), (2.2), and (2.5) can be written as

$$-\nabla\cdot(\epsilon\nabla\phi) = q_p C_p + \textstyle\sum_i q_i \widehat{C}_i \exp(-\beta_i(\phi+\psi_i^{\pm})), \tag{2.9}$$

$$\frac{\mp\hbar^2}{2m_i}\Delta\sqrt{C_i} = \sqrt{C_i}\left[\frac{-1}{\beta_i}\left(\ln\left(\sqrt{C_i}\right)^2 - \ln\widehat{C}_i\right) - \phi\right], \tag{2.10}$$

$$\nabla\cdot\left[D_i\exp(-\beta_i(\phi+\psi_i^{\pm}))\nabla\widehat{C}_i\right] = 0. \tag{2.11}$$

Note that all these three elliptic PDEs are self-adjoint with respect to the three unknown functions ϕ, $\sqrt{C_i}$, and $\widehat{C}_i$ and that the first two are semilinear. Here all functions are defined in R^3 such as $\phi(\mathbf{r})$, $\mathbf{r}\in\Omega\subset R^3$, where Ω is the domain of the functions. The new variable $\widehat{C}_i$ is an extension of the classical Slotboom variable [31] to include the quantum potential $\psi_i^{\pm}$ and thus called a quantum Slotboom variable.

3 A Generalized Gummel Algorithm and Numerical Methods

The classical Gummel iteration developed in [15] is to decouple the drift-diffusion equations and solve them in a successive and iterative manner. With the additional equation (2.10) for the QCPNP model, we generalize Gummel's algorithm as follows.

Step 1. Choose initial guesses $\widehat{C}_i^{(0)}$ and $\psi_i^{\pm(0)} = 0$, $\forall i$.

Step 2. Solve for $\phi^{(1)}$ the semilinear PDE

$$-\nabla\cdot(\epsilon\nabla\phi^{(1)}) = q_p C_p + \textstyle\sum_i q_i \widehat{C}_i^{(0)} \exp(-\beta_i(\phi^{(1)}+\psi_i^{\pm(0)})). \tag{3.1}$$

Step 3. Solve for $\sqrt{C_i}^{(1)}$ the semilinear PDE

$$\frac{\mp\hbar^2}{2m_i}\Delta\sqrt{C_i}^{(1)} = \sqrt{C_i}^{(1)}\left[\frac{-1}{\beta_i}\left(\ln\left(\sqrt{C_i}^{(1)}\right)^2 - \ln\widehat{C}_i^{(0)}\right) - \phi^{(1)}\right], \quad \forall i. \tag{3.2}$$

Step 4. Solve for $\widehat{C}_i^{(1)}$ the linear PDE

$$\nabla\cdot\left[D_i\exp(-\beta_i(\phi^{(1)}+\psi_i^{\pm(0)}))\nabla\widehat{C}_i^{(1)}\right] = 0, \quad \forall i. \tag{3.3}$$

Step 5. Update

$$\psi_i^{\pm(0)} = \frac{-1}{\beta_i}\left(\ln\left(\sqrt{C_i}^{(1)}\right)^2 - \ln\widehat{C}_i^{(1)}\right) - \phi^{(1)}, \quad \widehat{C}_i^{(0)} = \widehat{C}_i^{(1)}, \quad \forall i, \tag{3.4}$$

and go to Step 2 if necessary.

Note that the boundary conditions (of Dirichlet type) associated with (3.1), (3.2), and (3.3) are not specified in the algorithm and will be given in the next section. Due to the exponential function, Eq. (3.3) is usually discretized by combining the Scharfetter-Gummel method [29] and the finite element method [7].

The present algorithm does not include the inner iteration loop introduced in [10], which combines Steps 2 and 3 to form a single step of a coupled system of the nonlinear problems (3.1) and (3.2) and thus requires an inner iteration to decouple the system for numerical implementation, since we do not compute exclusively the intermediate quantum Slotboom variables via quasi-Fermi potentials. There is no quasi-Fermi potential for ion channel models. The quantum Slotboom variables $\widehat{C}_i$ defined in (2.6) are in fact the primary variables in our algorithm just like the classical Slotboom variables used in the original Gummel algorithm for the self-adjoint drift-diffusion model [31].

The convergence analysis of the semilinear PDEs (3.1) and (3.2) in discrete form can be extended from that of the QC energy transport model of semiconductor devices presented in [9], where the linear system of algebraic equations is shown to be an M-matrix, the convergence rate of a monotone iterative method for the nonlinear algebraic systems is shown to be optimal in the sense of Gummel's decoupling iteration, and the method is globally convergent if the initial guess is taken to be a lower or an upper solution of the nonlinear algebraic system. However, the functional analysis on the questions of existence, multiple solutions, and uniqueness of these semilinear PDEs with practical biasing voltages remains open.

4 Numerical Results of the K Channel

For numerical verification, we consider the K channel of [14] as shown in Fig. 1, where the length and radius of the channel are $l_c = 3.5$ and $r_c = 0.5$ nm, respectively, and $l_b = 5$ and $r_b = 5.5$ nm are the length and radius of the interior and exterior baths, respectively. Since the domain is in a dumbbell shape, the 3D QCPNP model can be reduced to a 1D model as

$$-\frac{d}{dz}\left(A\epsilon\frac{d\phi}{dz}\right) = q_p C_p + \sum_i q_i \widehat{C}_i \exp(-\beta_i(\phi + \psi_i^{\pm})), \tag{4.1}$$

$$\frac{\mp\hbar^2}{2m_i}\frac{d}{dz}\left(A\frac{d\sqrt{C_i}}{dz}\right) = \sqrt{C_i}\left[\frac{-1}{\beta_i}\left(\ln\left(\frac{\sqrt{C_i}}{A}\right)^2 - \ln\frac{\widehat{C}_i}{A}\right) - \phi\right], \tag{4.2}$$

$$\frac{d}{dz}\left(\left[D_i\exp(-\beta_i(\phi+\psi_i^{\pm})\right]\frac{d}{dz}\frac{\widehat{C}_i}{A}\right) = 0, \tag{4.3}$$

with the boundary conditions

$$\phi(-l) = 0, \quad \phi(l) = V, \tag{4.4}$$

$$\sqrt{C_i}(\pm l) = \sqrt{C_{bi}}, \tag{4.5}$$

$$\widehat{C}_i(-l) = C_{bi}, \quad \widehat{C}_i(l) = \exp(\beta_i V)C_{bi}, \tag{4.6}$$

where the relations between 3D and 1D functions are $\phi(\mathbf{r}) = \phi(z)$, $\psi_i^{\pm}(\mathbf{r}) = \psi_i^{\pm}(z)$, $\sqrt{C_i}(\mathbf{r}) = \sqrt{C_i}(z)/A(z)$, $\widehat{C}_i(\mathbf{r}) = \widehat{C}_i(z)/A(z)$, $C_p(\mathbf{r}) = C_p(z)/A(z)$, $C_p(\mathbf{r}) = C_p(z)/A(z)$ with $-l \le z \le l$, $l = l_b + l_c/2$, V is the applied voltage, and C_{bi} is the concentration of ion species i in the bath. Here $A(z)$ is the cross sectional area of the solvent domain that is transformed from the dumbbell shape to a funnel shape as $A(z) = \pi r_c^2$ for $z \in [-l_c/2, +l_c/2]$ and $A(z)$ varies linearly with z from πr_c^2 at $z = \pm l_c/2$ to πr_b^2 at $z = \pm l$.

For different regions of the K channel and surrounding KCl baths, the physical constants of various parameters are given in Table 1 where the units of the mobility μ, the diffusion coefficient D, and the bath concentration C_{bi} are $10^{-5}\text{cm}^2/\text{(Vs)}$, 10^{-5} cm^2/s, and molar, respectively. The bath concentrations for the positive and negative ions are 0.15 molar = 9×10^{19} cm^{-3}. The concentration of charged atoms in the protein $C_p(\mathbf{r})$ is defined as a step function shown in Fig. 2, where the vertical scale is $\log_{10}$ of concentration/$(10^{21}$ $\text{cm}^{-3})$.

Numerical simulations of this channel problem were carried out by both PNP (omitting $\psi_i^{\pm}$ and (3.2)) and QCPNP models for comparison. With $V = -100$ mV, the computed ion concentrations are shown in Figs. 2 and

Table 1: Physical constants.

Region	l	ϵ	μ	D	q_p
Baths	5	80	60	1.5	0
-4e group	0.2	80	16	0.4	$-4e$
Nonpolar	1.1	4	16	0.4	0
Central Cavity	1	30	16	0.4	$-0.5e$
Filter	1.2	30	16	0.4	$-1.5e$

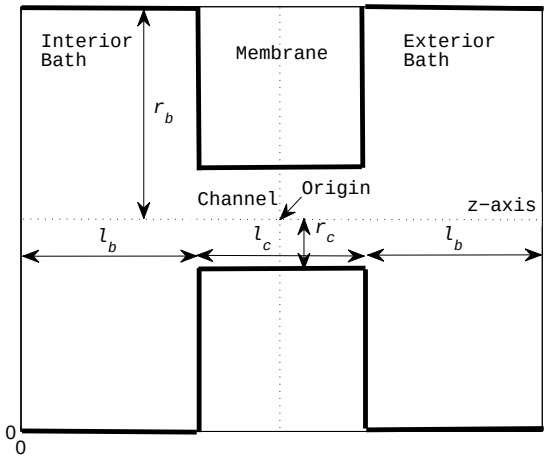

Figure 1: Geometry of K channel, membrane, and interior and exterior baths.

Table 2: Average number of ions in channel.

Method	K^+	Cl^-
PNP	4.58	0.91
QCPNP	4.48	0.77
Experiment	4.3	0

3. We first note that numerical results obtained by the PNP model are almost identical to that of [14] where the time-dependent PNP model is used. From Table 2, we see that the average number of ions predicted by the QCPNP model is more consistent with the charge structure of the protein known from the experimental X-ray crystallography [14] than that predicted by the PNP model under the same simulation parameters and conditions although the difference is small. It therefore justifies that the QCPNP model is a more refined and accurate model. The ion flow is from the interior (left) to the exterior (right) of the cell membrane. PNP predicts $I^+ = 24.24$ pA (pico Amperes) for the K^+ current in the channel and $I^- = 0.39$ pA for the Cl^- current whereas QCPNP yields $I^+ = 22.68$ pA and $I^- = 0.31$ pA. The total current is reduced about 6.6% by the QCPNP model.

Furthermore, significant differences in electrostatic potential calculated by PNP and QCPNP models are shown in Fig. 4, especially around the local extreme points of the potential profile. The difference between two cases relative to the potential obtained by QCPNP is 8.3% at the first (left) valley in Fig. 4, while it is 19% at the peak. These extreme points are a direct consequence of the -4e group in Table 1 (around $z = 0$ in Fig. 1) that we use to model the charged vestibule in the channel mouth, which attracts K^+ ions and hence increases the local vestibule concentration and causes the large variation of the potential within this very narrow region (0.2 nm in our model). It is well known that charged vestibules have been shown to play a significant role in the permeation of ions through biological ion channel [5, 19]. These expressive differences are of course due to the quantum potentials (2.3) and (2.4) that we have added to the standard PNP model. The QCPNP model may thus offer a different perspective from the PNP theory on modeling ion-selective ligand-gated or voltage-activated channels for which the role of charged vestibules is prominent. These results also indicate that the QCPNP model may be considered as a more refined continuum model that can be incorporated into a multi-scale electrophysiology modeling from the molecular motions of ion channels to the whole cell physiology [12, 30].

Gummel's iterative method has been shown analytically and numerically to yield convergent results from a lower or upper solution of the QC energy transport model in [9]. Table 3 shows that the method con-

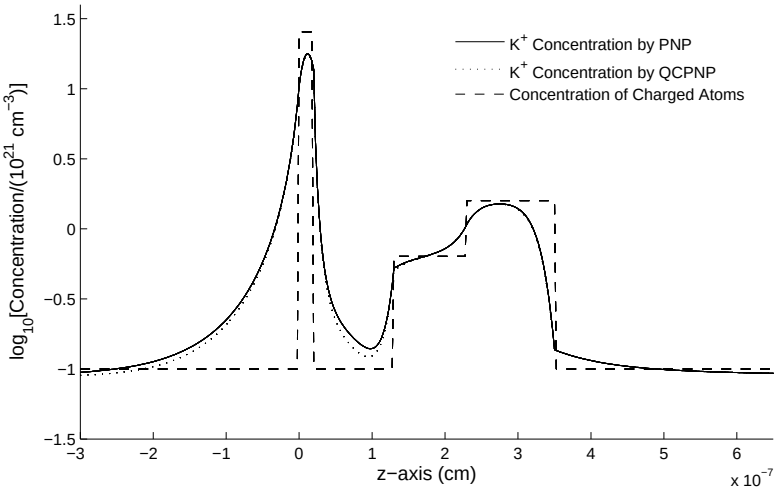

Figure 2: K^+ concentrations computed by PNP (solid line) and QCPNP (dotted line) models with the concentration of charged atoms in the protein (dashed line).

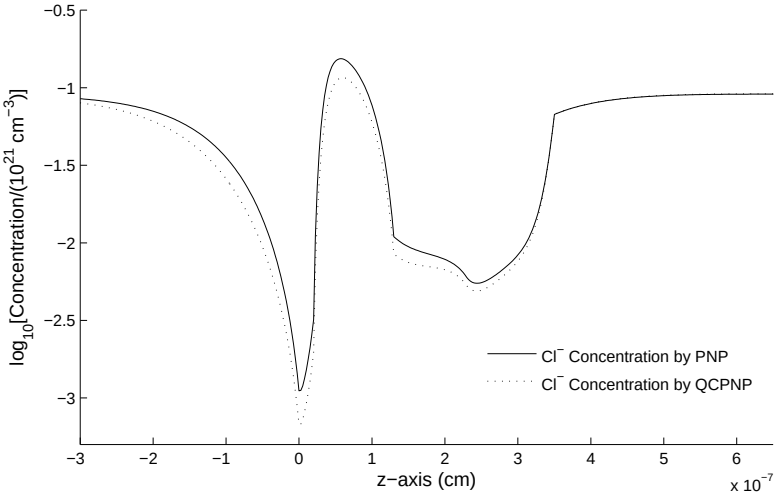

Figure 3: Cl^- concentrations computed by PNP (solid line) and QCPNP (dotted line) models.

verges quite effectively as well for the present QCPNP model, where Error = $\left\|\phi^{(k)} - \phi^{(k-1)}\right\|_\infty$ with $\left\|\phi^{(k)}\right\|_\infty = \max_i \left|\phi_i^{(k)}\right|$ being the maximum absolute value of the approximate potential function $\phi^{(k)}(z)$ over all grid points z_i in the domain at k^{th} iterate, for $k = 1, 2, \cdots$, with a suitable initial guess of $\phi(z)$ [9].

We make a final remark on the extension of the QCPNP to more realistic channel proteins in 3D and dynamical implementations. Taking account of the steric effect of ions and water with nonuniform sizes, the correlation effect of crowded ions with different valences, and the polarization effect of water molecules, an advanced theory — called Poisson-Nernst-Planck-Fermi theory — has been developed by Liu and Eisenberg in a series of recent papers [23–28], where a variety of applications to ion channels, electric double layers, and ion activity in water have been investigated by this theory. As shown in [23, 27], the 3D implementation of continuum models like PNP, PNPF, or QCPNP for real protein channels is very challenging due to a wide range of numerical issues such as the geometric singularities of molecular surface, the singular charges in real proteins, the complex and large simulation domain containing protein channels, the strong nonlinear nature of

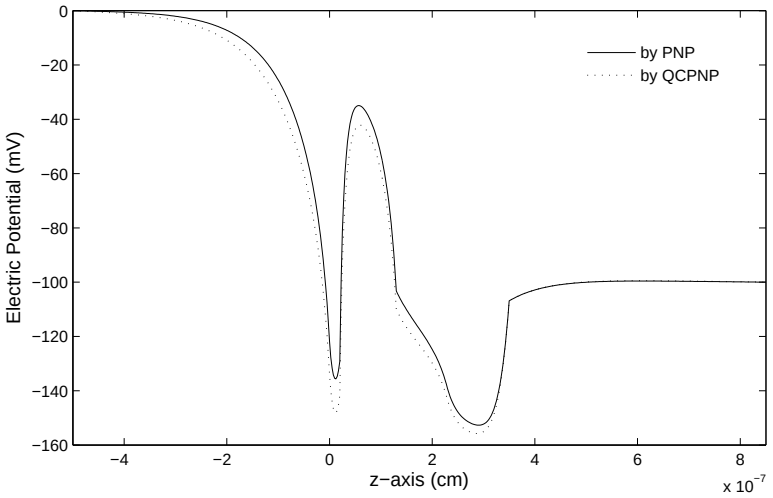

Figure 4: Electrostatic potential computed by PNP (solid line) and QCPNP (dotted line) models.

Table 3: Convergence of Gummel's Iteration.

Iterate	1	2	3	4	5
Error	0.1324	0.0662	0.0261	0.0096	0.0018

the biological system, and a very large range of applied voltages and bath concentrations in experimental or physiological conditions. The additional QC equations (2.10) would certainly make the 3D implementation more complicated and time consuming. Nevertheless, all PNP, PNPF, and QCPNP models are of elliptic type of PDEs in steady state. Standard numerical methods such as the finite difference method, fast linear and nonlinear solvers, and effective time discretization methods can all be utilized to explore a great variety of physical and chemical properties described by these advanced continuum models that offer much more comprehensive and efficient simulations of biological systems than molecular dynamics, Brownian dynamics, or Monte Carlo simulations.

5 Conclusion

A quantum corrected Poisson-Nernst-Planck model is proposed for biological ion channels. It is shown to be more refined and accurate than the classical one and may be useful to study ion-selective ligand-gated or voltage-activated channels for which the role of highly charged vestibules is prominent. The present results illustrate notable differences between quantum and electrostatic potentials. It will be interesting to include the quantum effect in the Poisson-Nernst-Planck-Fermi theory recently developed for modeling realistic channel proteins in which the steric and correlation effects of ions and water have been shown to play important roles in properly describing various experimental results.

Acknowledgement: This work was supported by the Ministry of Science and Technology, Taiwan (MOST 103-2115-M-134-004-MY2). The author is grateful to R.-C. Chen and H.-H. Wu for the help on computational work in this paper.

Conflict of interest: Author state no conflict of interest.

References

[1] U. Ascher, P. Markowich, C. Schmeiser, H. Steinruck, and R. Weiss, Conditioning of the steady state semiconductor device problem, SIAM J. Appl. Math. 49 (1989) 165-185.

[2] V. Barcilon, D. P. Chen, and R. S. Eisenberg, Ion flow through narrow membrane channels: Part II, SIAM J. Appl. Math. 53 (1992)1405-1425.

[3] D. Bohm, A suggested interpretation of the quantum theory in terms of hidden variables I and II, Phys. Rev., 85 (1952), pp. 166-179 and 180-93.

[4] F. Brezzi, L. D. Marini, and P. Pietra, Two-dimensional exponential fitting and applications to drift-diffusion models, SIAM J. Numer. Anal. 26 (1989) 1342-1355.

[5] M. Cai and P. C. Jordan, How does vestibule surface charge affect ion conduction and toxin binding in a sodium channel? Biophys. J. 57 (1990) 883-891.

[6] D. P. Chen and R. S. Eisenberg, Charges, currents and potentials in ionic channels of one conformation, Biophys. J. 64 (1993) 1405-1421.

[7] R.-C. Chen and J.-L. Liu, An iterative method for adaptive finite element solutions of an energy transport model of semiconductor devices, J. Comput. Phys. 189 (2003) 579-606.

[8] R.-C. Chen and J.-L. Liu, A quantum corrected energy-transport model for nanoscale semiconductor devices, J. Comput. Phys. 204 (2005) 131-156.

[9] R.-C. Chen and, J.-L. Liu, An accelerated monotone iterative method for the quantum-corrected energy transport model, J. Comp. Phys. 227 (2008) 6266-6240.

[10] C. de Falco, J. W. Jerome, and R. Sacco, Quantum corrected drift-diffusion models: Solution fixed point map and finite element approximation, J. Comput. Phys., 228 (2009), pp. 1770-1789.

[11] R. Eisenberg, From structure to function in open ionic channels, J. Membr. Biol. 171 (1999) 1-24.

[12] R. Eisenberg, Multiple scales in the simulation of ion channels and proteins, J. Phys. Chem. C 114 (2010) 20719-20733.

[13] B. Eisenberg, Y. Hyon, and C. Liu, Energy variational analysis EnVarA of ions in water and channels: Field theory for primitive models of complex ionic fluids, J. Chem. Phys. 133 (2010) 104104.

[14] C. L. Gardner, W. Nonner and R. S. Eisenberg, Electrodiffusion model simulation of ionic channels: 1D simulations, J. Comput. Electronics 3 (2004) 25-31.

[15] H. K. Gummel, A self-consistent iterative scheme for the one-dimensional steady-state transistor calculations, IEEE Trans. Elec. Dev. ED-11 (1964) 163-174.

[16] B. Hille, Ionic Channels of Excitable Membranes, 3rd Ed., Sinauer Associates Inc., Sunderland, MA, 2001.

[17] P. R. Holland, The Quantum Theory of Motion, Cambridge University Press, 1993.

[18] T.-L. Horng, T.-C. Lin, C. Liu, and B. Eisenberg, PNP equations with steric effects: a model of ion flow through channels, J. Phys. Chem. B 116 (2012) 11422-11441.

[19] M. Hoyles, S. Kuyucak, and S.-H. Chung, Energy barrier presented to ions by the vestibule of the biological membrane channel, Biophys. J. 70 (1996) 1628-1642.

[20] J. W. Jerome, Consistency of semiconductor modeling: An existence/stability analysis for the stationary van Roosbroeck system, SIAM J. Appl. Math. 45 (1985) 565-590.

[21] T. Kerkhoven, A proof of convergence of Gummel's algorithm for realistic device geometries, SIAM J. Numer. Anal. 23 (1986) 1121-1137.

[22] Y. Li, J.-L. Liu, S.M. Sze, and T.-S. Chao, A new parallel adaptive finite volume method for the numerical simulation of semiconductor devices, Comput. Phys. Commun. 142 (2001) 285-289.

[23] J.-L. Liu, Numerical methods for the Poisson-Fermi equation in electrolytes, J. Comput. Phys. 247 (2013) 88-99.

[24] J.-L. Liu and B. Eisenberg, Correlated ions in a calcium channel model: a Poisson-Fermi theory, J. Phys. Chem. B 117 (2013) 12051-12058.

[25] J.-L. Liu and B. Eisenberg, Analytical models of calcium binding in a calcium channel, J. Chem. Phys. 141 (2014) 075102.

[26] J.-L. Liu and B. Eisenberg, Poisson-Nernst-Planck-Fermi theory for modeling biological ion channels, J. Chem. Phys. 141 (2014) 22D532.

[27] J.-L. Liu and B. Eisenberg, Numerical methods for a Poisson-Nernst-Planck-Fermi model of biological ion channels, Phys. Rev. E 92 (2015) 012711.

[28] J.-L. Liu and B. Eisenberg, Poisson-Fermi model of single ion activities in aqueous solutions, Chem. Phys. Lett. 637 (2015) 1-6.

[29] D. L. Scharfetter and H. K. Gummel, Large-signal analysis of a silicon Read diode oscillator, IEEE Trans. Elec. Dev. ED-16 (1969) 64-77.

[30] J. R. Silva and Y. Rudy, Multi-scale electrophysiology modeling: from atom to organ, J. Gen. Physiol. 135 (2010) 575-581.

[31] J. W. Slotboom, Computer-aided two-dimensional analysis of bipolar transistors, IEEE Trans. Elec. Dev. ED-20 (1973) 669-679.